Neuron, Vol. 38, 253–263, April 24, 2003, Copyright ©2003 by Cell Press

Circadian Dynamics of Cytosolic and Nuclear Ca^{2+} in Single Suprachiasmatic Nucleus Neurons

Masayuki Ikeda,[1,2,3,*] Takashi Sugiyama,[2] Christopher S. Wallace,[3] Heinrich S. Gompf,[3] Tohru Yoshioka,[2] Atsushi Miyawaki,[4] and Charles N. Allen[3]

[1]Department of Molecular Behavioral Biology
Osaka Bioscience Institute
6-2-4 Furuedai, Suita
Osaka 565-0874

[2]Advanced Research Institute
for Science and Engineering
Waseda University
3-4-1 Okubo, Shinjyuku-ku
Tokyo 169-8555
Japan

[3]Center for Research on Occupational and Environmental Toxicology
Oregon Health & Science University
Portland, Oregon 97201

[4]Cell Function and Dynamics
Brain Science Institute
RIKEN
2-1 Hirosawa, Wako
Saitama 351-0198
Japan

Summary

Intracellular free Ca^{2+} regulates diverse cellular processes, including membrane potential, neurotransmitter release, and gene expression. To examine the cellular mechanisms underlying the generation of circadian rhythms, nucleus-targeted and untargeted cDNAs encoding a Ca^{2+}-sensitive fluorescent protein (cameleon) were transfected into organotypic cultures of mouse suprachiasmatic nucleus (SCN), the primary circadian pacemaker. Circadian rhythms in cytosolic but not nuclear Ca^{2+} concentration were observed in SCN neurons. The cytosolic Ca^{2+} rhythm period matched the circadian multiple-unit-activity (MUA)-rhythm period monitored using a multiple-electrode array, with a mean advance in phase of 4 hr. Tetrodotoxin blocked MUA, but not Ca^{2+} rhythms, while ryanodine damped both Ca^{2+} and MUA rhythms. These results demonstrate cytosolic Ca^{2+} rhythms regulated by the release of Ca^{2+} from ryanodine-sensitive stores in SCN neurons.

Introduction

The hypothalamic suprachiasmatic nucleus (SCN) in mammals functions as the primary circadian clock (Moore and Eichler, 1972; Stephan and Zucker, 1972). The SCN contains approximately 8000 neurons (van den Pol, 1980) that fire action potentials (Inouye and Kawamura, 1979; Green and Gillette, 1982) and secrete arginine-vasopressin and vasoactive intestinal peptide in approximately 24 hr cycles (Earnest and Sladek, 1986; Shinohara et al., 1995). The basic mechanism responsible for the rhythm generation is intrinsic to individual neurons because dispersed SCN neurons retain the firing rhythm with individual circadian frequencies (Welsh et al., 1995). SCN neurons grown as organotypic cultures exhibit firing rhythms with identical circadian frequencies (Herzog et al., 1997), suggesting neuronal synchronization in SCN circuits. The core molecular elements of the clock appear to be the transcription and translation feedback loops of "clock genes" (Shearman et al., 2000). The intracellular messengers by which the clock genes produce the firing and secretory rhythms, however, are not well understood.

Intracellular free Ca^{2+} regulates diverse cellular processes, including membrane potential, neurotransmitter release, and gene expression, and thus is one of the candidate intracellular messengers in the circadian system. Although rhythmic changes in cytosolic free Ca^{2+} concentration ($[Ca^{2+}]_c$) have been observed in tobacco and *Arabidopsis* plants (Johnson et al. 1995; Wood et al., 2001) by photon-counting analysis of aequorin chemiluminescence, little is known of the circadian $[Ca^{2+}]_c$ dynamics in single SCN neurons.

The steady-state $[Ca^{2+}]_c$ levels in the SCN have been estimated using fura-2AM-based Ca^{2+} imaging, and the population mean $[Ca^{2+}]_c$ in SCN cells was found to be higher during the daytime than the nighttime (Colwell, 2000). It was proposed that action potentials and voltage-gated Ca^{2+} channel activation might drive the circadian $[Ca^{2+}]_c$ rhythm because the day-night difference in $[Ca^{2+}]_c$ was blocked by the voltage-gated Na^+ channel blocker, tetrodotoxin (TTX), and the voltage-sensitive Ca^{2+} channel blocker, methoxyverapamil (Colwell, 2000). Using a similar experimental strategy, however, we did not observe a day-night difference in the population mean $[Ca^{2+}]_c$ in SCN cells (Ikeda et al., 2003). Both of these studies compared different SCN cells sampled in different slices during either the day or night, since fura-2 can not be used to follow the $[Ca^{2+}]_c$ of single cells over a complete circadian cycle.

To examine progressive changes in free Ca^{2+} concentration in single SCN neurons for multiple circadian cycles, therefore, we used the Ca^{2+}-sensitive fluorescent protein cameleon (Miyawaki et al., 1997, 1999) expressed in organotypic SCN cultures with a neuron-specific enolase promoter (Sakimura et al., 1995). The improved cameleon (YC2.1), which is significantly less sensitive to pH than the original cameleon, has been successfully used in primary cultures of hippocampal and cortical neurons (Miyawaki et al., 1999; Tsuchiya et al., 2002). Also, this Ca^{2+} indicator has been stably expressed in *C. elegans* neurons (Kerr et al., 2000), demonstrating its applicability for the long-term monitoring of neuronal $[Ca^{2+}]_c$. The present results demonstrate a circadian rhythm of the cytosolic but not nuclear Ca^{2+} concentration in SCN neurons. The $[Ca^{2+}]_c$ rhythm was not blocked by TTX, indicating that this rhythm was not dependent on action potential firing. Rather, the simultaneous monitoring of firing rhythms using a multiple-electrode-array dish (MEAD) raised the possibility

*Correspondence: msikeda@obi.or.jp

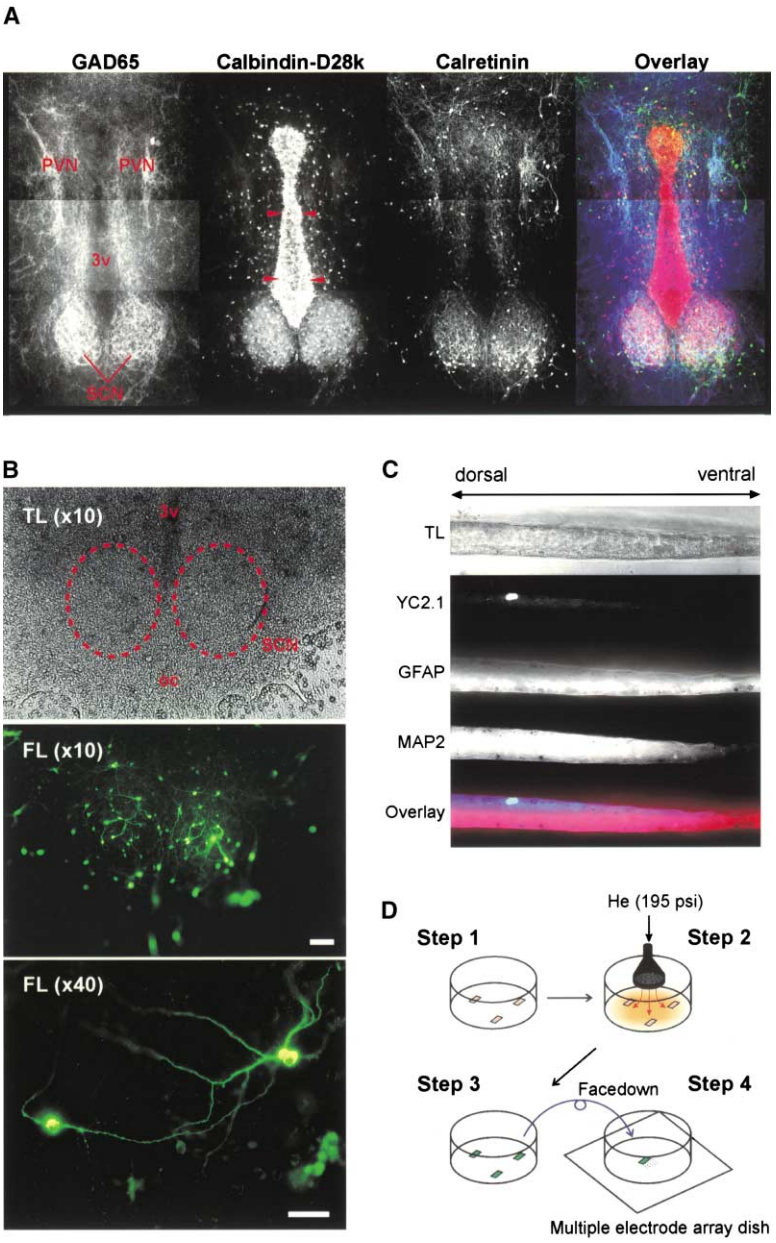

Figure 1. Making of Cameleon-Expressing SCN Slice Cultures

(A) Immunostaining of a mouse hypothalamic slice culture with antibodies against GAD65 (blue), calbindin-D28k (red), and calretinin (green). Higher levels of GAD65 and calbindin were observed in the SCN than in the surrounding areas. Periventricular tanycyte-like cells (arrow heads) also exhibited significant calbindin expression. Calretinin was distributed throughout the ventral SCN.

(B) A living hypothalamic slice culture expressing cameleon, viewed using a 10× objective lens (TL [10×], transmitted light image; FL [10×], fluorescent light image, bar = 100 μm) and 40× objective lens (FL [40×], bar = 30 μm).

(C) Immunostaining of a cameleon (YC2.1, green)-expressing slice with antibodies for MAP2 (blue) and GFAP (red). The slice culture was sectioned perpendicular to the top of the culture. The GFAP-immunoreactive astrocytes were located primarily on the bottom, while MAP2-immunoreactive neurons were located primarily through the middle to the top surface. The maximal slice thickness was approximately 50 μm. Cameleon-expressing neurons were located at the surface.

(D) The strategy for transfection of the cameleon gene into hypothalamic slices and placement onto the MEAD. Step 1: 7- to 9-day-old slice cultures were grown on membrane filters. Step 2: gene-gun transfection with vector-coated gold particles and 195 psi helium gas pressure. Step 3: expression of cameleon protein 3–5 days after Step 2. Step 4: selection and placement of SCN slice onto the electrode array.

that $[Ca^{2+}]_c$ rhythms indirectly drive the circadian rhythmicity of action potential firing in SCN neurons.

Results

Immunohistochemical Characterization of SCN Slice Cultures

SCN slice cultures were characterized immunohistochemically for the presence of an enzyme involved in the synthesis of GABA, glutamic acid decarboxylase-65 kDa (GAD65), and two Ca^{2+} binding proteins, calbindin D28k and calretinin (Figure 1A). GAD65-immunoreactive neurons were densely expressed in the SCN, sending efferent fibers parallel to the third ventricle and into the paraventricular nucleus. Extensive calbindin immunoreactivity was observed throughout the SCN and in periventricular tanycyte-like cells. Ventral SCN and a subpopulation of paraventricular nucleus neurons were calretinin immunoreactive. Thus, many ventral SCN neurons were immunoreactive for both calbindin and calretinin.

Cameleon cDNA linked to the neuron-specific enolase promoter was transfected into SCN slice cultures using a gene gun (Figures 1B–1D). Cameleon was expressed primarily in neurons, although several glial cells on the ventral edge of the slice also expressed cameleon. The transfection protocol was optimized so that the number of transfected SCN neurons was small, enabling visualization of individual neurons (Figure 1B). Because the permeability of gold particles carrying the cDNA vector was limited, cameleon expression was confined to neurons near the slice surface, where microtubule associated protein-2 (MAP2)-immunoreactive neurons but not glial fibrillary acidic protein (GFAP)-immunoreactive

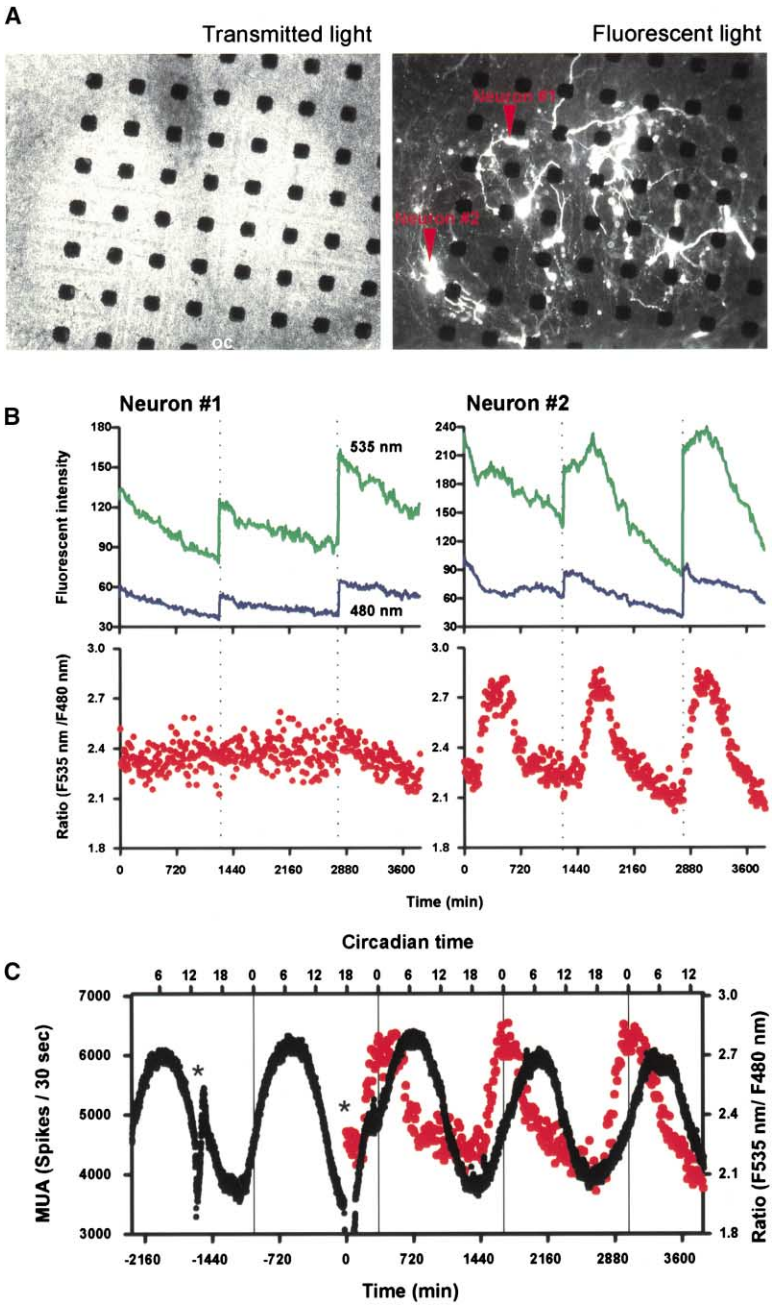

Figure 2. Long-Term Cytosolic Ca^{2+} Imaging on the Multiple Electrode Array

(A) Images of a living SCN slice cultured on a MEAD with transmitted light (left) and fluorescent light (right) were viewed using an inverted microscope. Each electrode consisted of 20 × 20 μm platinum black connected to transparent indium tin oxide leads.

(B) Long-term measurement of emission intensities at 535 nm (green) and at 480 nm (blue) from untargeted cameleon expressed in two SCN neurons. Broken lines indicate the resetting of the dynamic range with an image intensifier. Neuron #1 located in the dorsomedial SCN exhibited no oscillation in the emission ratio (F535 nm/F480 nm), while neuron #2 located in the ventrolateral SCN exhibited circadian oscillations.

(C) Simultaneous recording of MUA demonstrated that the MUA rhythm had a period identical to that of the $[Ca^{2+}]_c$ rhythm. MUA was recorded using a pair of electrodes in the middle of the left SCN, although MUA rhythms recorded with any electrode combination exhibited identical circadian periodicity in the slice. The peak of the $[Ca^{2+}]_c$ rhythm of neuron #2 was 6 hr advanced from that of the MUA rhythm. Asterisks indicate the timing of the culture medium exchange, during which the firing frequency became temporarily unstable. Time 0 denotes initiation of fluorescence measurement.

astrocytes were clustered (Figure 1C). After successful transfection of cameleon cDNA into living SCN neurons, the cameleon-expressing surface was placed on the collagen-coated MEAD to record action potentials (Figures 1D and 2A).

Cytosolic Ca^{2+} Dynamics in SCN Neurons

SCN neurons expressing the untargeted cameleon were placed in an environmentally regulated chamber, and $[Ca^{2+}]_c$ and multiunit activity (MUA) were simultaneously recorded. $[Ca^{2+}]_c$ was estimated from the reciprocal emission intensity changes at 480 and 535 nm produced by the fluorescent resonance energy transfer in the Ca^{2+}-bound cameleon molecule. The $[Ca^{2+}]_c$ in the majority of SCN neurons (64%, 89 of 139) changed in a circadian pattern from a mean baseline ratio of 2.31 ± 0.04 to a mean peak ratio of 2.75 ± 0.05 (Figure 2B). The mean period of the $[Ca^{2+}]_c$ rhythms was 23.8 ± 0.2 hr (n = 89). Chelation of Ca^{2+} with EGTA and BAPTA-AM (30 μM) reduced the mean ratio to minimal levels (R_{min} = 1.75 ± 0.02, n = 16) while the Ca^{2+} ionophore, ionomycin (3 μM), elevated the mean ratio to maximal levels (R_{max} = 3.16 ± 0.05, n = 16). From the primary dissociation constant of cameleon (K_{d1} = 100 nM), the mean $[Ca^{2+}]_c$ was estimated to be 119 ± 2 nM at the circadian nadir and 440 ± 8 nM at the peak. Neurons and glial cells located outside of the SCN and 36% of SCN neurons (50 of 139) exhibited no changes in the

emission intensity ratio during a 24 hr period (mean Ca^{2+} concentration = 131 ± 4 nM; Figure 2B).

MUA was recorded via eight pairs of electrodes that were under and around the cameleon-expressing neurons. The MUA recorded at each electrode combination oscillated with identical circadian rhythms, suggesting a coupling of population firing rhythms within the SCN. The mean period of the MUA rhythm was 23.8 ± 0.3 hr (number of slices = 22), almost identical to that of the $[Ca^{2+}]_c$ rhythms (23.8 ± 0.2 hr). The peak of the $[Ca^{2+}]_c$ rhythm in the majority of neurons preceded the MUA peak (defined as circadian time 6; CT 6) by 2–7 hr (the mean $[Ca^{2+}]_c$ peak was at CT 1.6 ± 0.2 hr, n = 85; Figures 2C and 3A–3D). Four neurons in three slices exhibited $[Ca^{2+}]_c$ rhythms oscillating 180 degrees out of phase with the majority of the $[Ca^{2+}]_c$ rhythms (Figure 3D).

Several blockers of Ca^{2+} release from internal stores were used to analyze the role of internal Ca^{2+} stores in the generation of $[Ca^{2+}]_c$ and MUA rhythms. A 12 hr (CT 18-CT 6) treatment with an inositol (1,4,5)-trisphosphate (IP_3)-sensitive Ca^{2+} release blocker, thapsigargin (1 μM), resulted in a small increase of $[Ca^{2+}]_c$ at the onset, but had little effect on the $[Ca^{2+}]_c$ or MUA rhythms (n = 12, number of slices = 3; Figure 3A). Identical treatment with ryanodine (5 μM) resulted in an immediate increase in the $[Ca^{2+}]_c$ (76% ± 7% amplitude of the previous circadian cycle, n = 12) and then a successive decrease to the level of circadian nadir of the $[Ca^{2+}]_c$ rhythm (Figure 3A). The peak of MUA rhythms at the end of 5 μM ryanodine treatment (at CT 6) was 25% ± 4% smaller than the peak of control cycles (number of slices = 3, $p < 0.05$; Figures 3A and 3E). Ryanodine at a higher concentration (100 μM) for 12 hr (CT 18–CT 6) resulted only in a decrease in $[Ca^{2+}]_c$ levels and reduction of MUA peaks (Figure 3E; traces not shown). The reduction of $[Ca^{2+}]_c$ (−59% ± 12%, n = 12, $p < 0.01$) and MUA (−22% ± 8%, number of slices = 3, $p < 0.05$) rhythms was also confirmed by treatment with another blocker of Ca^{2+} release from ryanodine-sensitive stores, 8-bromo cyclic adenosine diphosphate-ribose (8-Br-cADPR, 300 μM), although washout of this drug was difficult.

An L-type Ca^{2+} channel blocker, nimodipine, and a voltage-gated Na^+ channel blocker, TTX, were used to analyze the role of voltage-dependent Ca^{2+} influx in the generation of $[Ca^{2+}]_c$ and MUA rhythms. The MUA rhythm peak (−68% ± 8%, number of slices = 3, $p < 0.01$) but not the $[Ca^{2+}]_c$ rhythm peak (−4% ± 6%, n = 12, n.s.) was significantly reduced after nimodipine treatment (2 μM for 5 hr; Figure 3C). TTX (0.5 μM) completely inhibited the MUA rhythms (−100% ± 0%, number of slices = 4, $p < 0.01$) but not the $[Ca^{2+}]_c$ rhythms (−2% ± 6%, n = 21, n.s.; Figures 3C and 3D). In addition, TTX treatment did not affect the anti-phase $[Ca^{2+}]_c$ rhythms (Figure 3D). Treatment with both nimodipine (2 μM) and TTX (0.5 μM) for more than one circadian cycle also had no effect on the $[Ca^{2+}]_c$ rhythm (−6% ± 5%, n = 12, n.s.; Figure 3C).

Nuclear Ca^{2+} Dynamics in SCN Neurons

We first compared receptor-mediated Ca^{2+} responses in slices expressing nucleus-targeted and untargeted cameleon. The expression of nucleus-targeted cameleon was limited to the nucleus with only faint leakage observed in the cytosol (Figure 4A). The nuclear cameleon exhibited a lower fluorescent ratio (−11.6% ± 3.8%, number of neurons = 4 in 4 separate slices, $p < 0.05$) than the cytosol (Figures 4B and 4C). The magnitude of NMDA-induced Ca^{2+} influx tended to be smaller in the nucleus (−38% ± 13%, n = 4 in separate slices, $p = 0.08$) than in the cytosol. Orphanin-FQ (300 nM), an agonist for a G protein-coupled receptor in the SCN, significantly reduced cytosolic (−6% ± 3%, $p < 0.05$), but not nuclear, Ca^{2+} concentrations (−1% ± 4%, n = 4 in separate slices, n.s.). Only the NMDA-induced Ca^{2+} increase in cytosol was significantly reduced by pretreatment with orphanin-FQ (−35% ± 16%, n = 4 in separate slices, $p < 0.05$).

The circadian dynamics of nuclear Ca^{2+} concentration were determined using nucleus-targeted cameleon together with MUA monitoring. Although the absolute intensity of fluorescence at 535 and 480 nm had an exponential bleaching decay as well as an occasional increase in intensity during continuous exposure to the excitation light, the intensity ratio was stable for more than two circadian cycles. No circadian oscillations in nuclear Ca^{2+} concentration (n = 24; Figures 5A and 5B) were detected in three slices with stable circadian MUA rhythms, while $[Ca^{2+}]_c$ exhibited circadian fluctuation in the majority of neurons (89 of 139 in 19 slices, 64%). The mean Ca^{2+} levels were significantly lower in the nucleus (35.2 ± 0.2 nM, n = 24) than the mean baseline Ca^{2+} levels in the cytosol (123.3 ± 0.9 nM, n = 139, pooled for rhythmic and nonrhythmic neurons, $p < 0.01$).

Discussion

The results of the present study show that Ca^{2+} levels in the cytosol but not the nucleus of SCN neurons exhibited a circadian rhythmicity. The $[Ca^{2+}]_c$ rhythm persisted in the presence of TTX, indicating that it was not dependent on the firing of action potentials. Moreover, the phase of the $[Ca^{2+}]_c$ rhythm led that of the MUA rhythm by 4.4 ± 0.2 hr on average. The $[Ca^{2+}]_c$ rhythm also persisted in the presence of a voltage-gated Ca^{2+} channel blocker, but was inhibited when release of Ca^{2+} from ryanodine-sensitive internal stores was blocked. These results demonstrate that cytosolic Ca^{2+} released from ryanodine-sensitive internal stores is a possible intracellular messenger involved in the generation of the circadian rhythmicity of SCN neuronal firing.

Cameleon Imaging in the Organotypic SCN Culture Plated on the MEAD

Organotypic cultures of the SCN were prepared from neonatal mice and maintained in vitro for up to 1 month. Because GABA is the principal neurotransmitter in the SCN (de la Mora et al., 1981; Moore and Speh 1993), the present study used GAD65 immunostaining to characterize the slice culture. The results revealed GAD65-immunoreactive SCN neurons sending efferent fibers to the paraventricular nucleus, consistent with the in vivo SCN or rat SCN slice cultures prepared using similar methods (Belenky et al., 1996). The GAD65-immunoreactive neurons maintained their composition to the end of the experiments, demonstrating that the integrity of the 2-dimensional SCN structure was maintained.

During the first few days in vitro, the number of GFAP-immunoreactive astrocytes significantly increased on

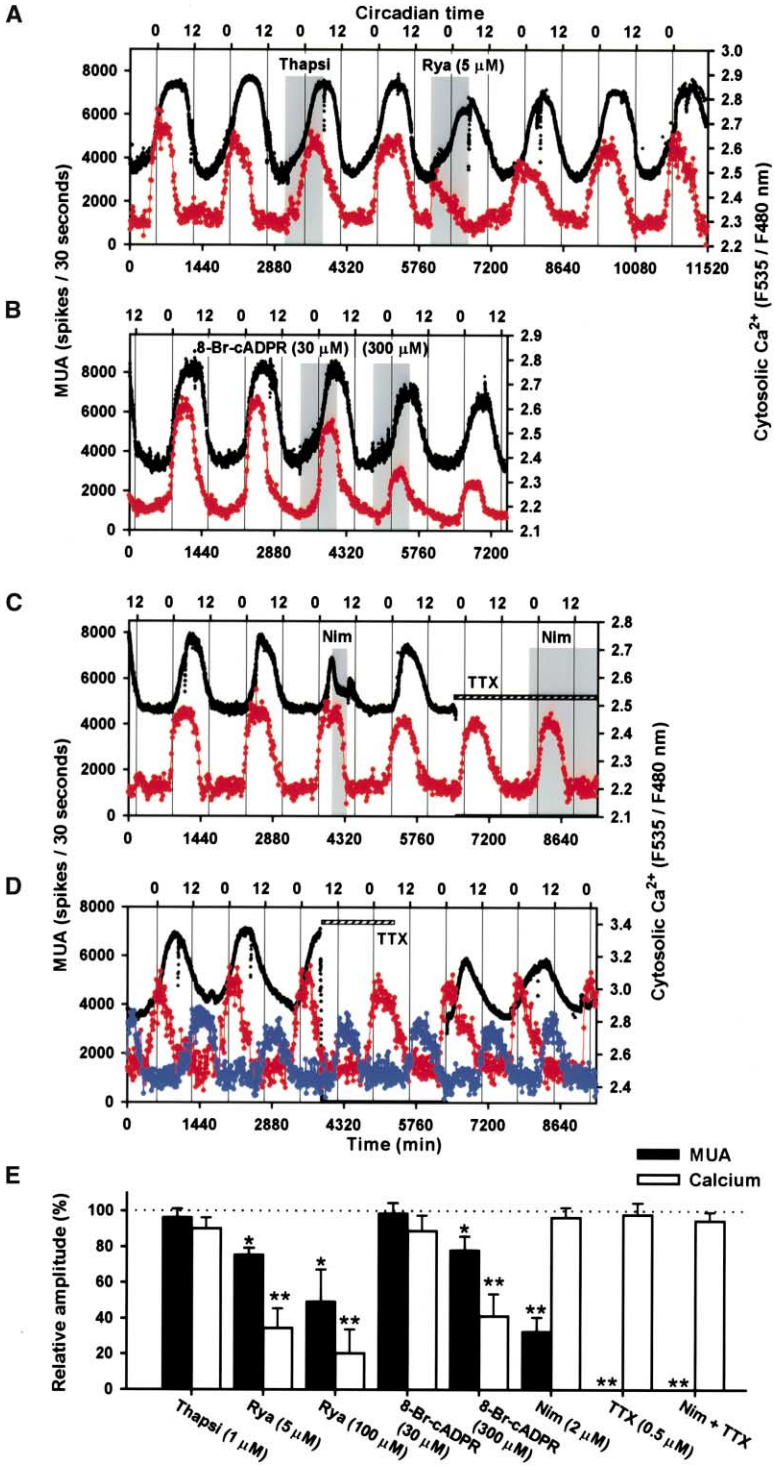

Figure 3. Circadian Cytosolic Ca^{2+} Rhythms Were Ryanodine- but Not TTX Sensitive

(A and B) The effects of internal Ca^{2+} store inhibitors on MUA (black) and $[Ca^{2+}]_c$ rhythms (red). (A) A 12 hr treatment with ryanodine (rya, 5 μM) but not thapsigargin (thapsi, 1 μM) reduced $[Ca^{2+}]_c$ and the peak MUA. Ryanodine at this concentration produced a transient increase and subsequent decrease in $[Ca^{2+}]_c$. (B) An inhibitor of ryanodine-sensitive Ca^{2+} stores, 8-bromo cyclic ADP ribose (8Br-cADPR, 300 μM), produced a reduction in $[Ca^{2+}]_c$ and a damping of the MUA rhythm.

(C and D) The effects of voltage-sensitive ion channel inhibitors on the MUA and $[Ca^{2+}]_c$ rhythms. (C) The L-type Ca^{2+} channel blocker, nimodipine (Nim, 2 μM), and the Na^+ channel blocker, TTX (0.5 μM), significantly reduced MUA frequency, while having little effect on $[Ca^{2+}]_c$. (D) Following the second washout of TTX, action potentials recovered almost in the same phase of the previous MUA rhythms. This slice contained a neuron with a $[Ca^{2+}]_c$ rhythm 180 degrees out of phase (blue).

(E) Mean peak amplitude of MUA and $[Ca^{2+}]_c$ rhythms were analyzed using a sine curve fitting. *$p < 0.05$, **$p < 0.01$ by paired t test in comparison with mean peak amplitudes before drug applications.

the bottom layer of the slice. The number of MAP2-immunoreactive neurons was reduced on the bottom layer of the slice culture, suggesting that astrocytes increased in parallel with the loss of neurons. This may produce technical difficulties for recording action potentials from slice cultures grown directly on planar electrode arrays. The 3-dimensional structure was stable after 1 week in vitro; thus, we replated the slice upside-down on the electrode arrays and were able to record cameleon fluorescence and action potentials in the same plane. Fluorescent signals from a limited layer such as this produce less scattering, enabling imaging using conventional (i.e., nonconfocal) microscopy.

Release of Ca^{2+} from Ryanodine-Sensitive Stores Is a Major Source of Circadian $[Ca^{2+}]_c$ Rhythms

Using the method proposed above, we observed stable circadian $[Ca^{2+}]_c$ rhythms in individual SCN neurons for periods of more than a week. IP_3-sensitive Ca^{2+} stores are present in SCN neurons (Kopp et al., 1999; Ikeda et

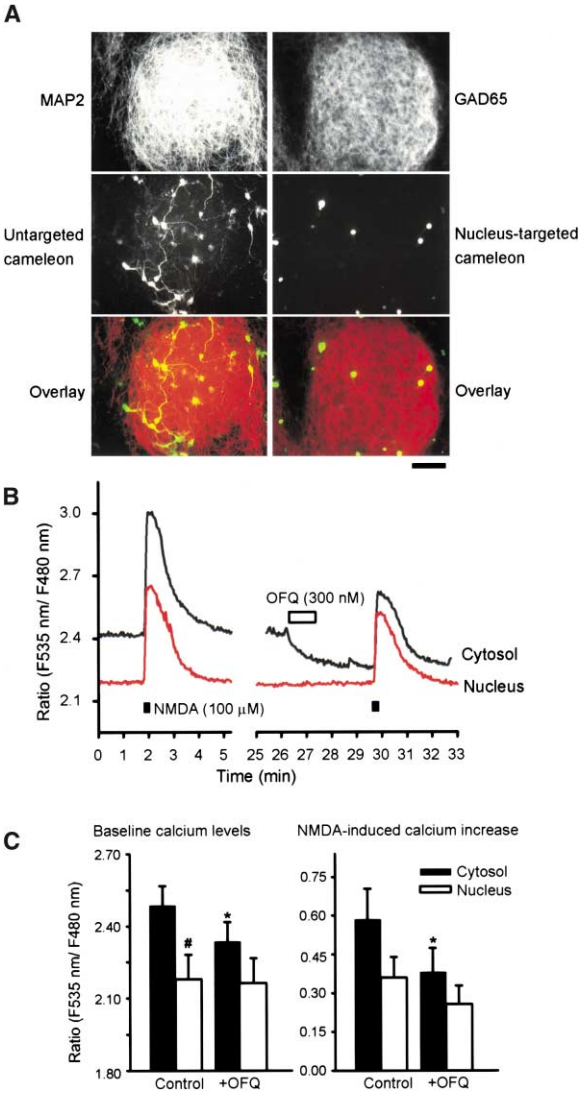

Figure 4. NMDA-Induced Ca^{2+} Mobilization in the Cytosol and Nucleus of SCN Neurons

(A) A cultured SCN slice transfected with untargeted cameleon cDNA (left) and a nucleus-targeted cameleon cDNA (right). MAP2 and GAD65 immunostaining (red in the overlay) was used to visualize the boundaries of the SCN. Scale bar = 100 μm.

(B and C) NMDA (100 μM) evoked mobilization of nuclear and cytosolic Ca^{2+} in a SCN neuron. Orphanin-FQ (300 nM) decreased baseline $[Ca^{2+}]_c$ and NMDA-induced Ca^{2+} influx in the cytosol. Nuclear Ca^{2+} concentrations were less sensitive to orphanin-FQ. This recording was conducted using an upright microscope with a 63× water immersion objective lens under the circulation of oxygen-saturated ACSF containing 1 μM TTX, 2.5 mM $CaCl_2$, and 0.5 mM $MgCl_2$. The mean Ca^{2+} response is shown in (C). OFQ, orphanin-FQ. #$p < 0.05$ in comparison with baseline $[Ca^{2+}]_c$ by unpaired t test; *$p < 0.05$ in comparison with corresponding controls by paired t test.

al., 2000), but the contribution of this Ca^{2+} store in the generation of the circadian $[Ca^{2+}]_c$ rhythm appears to be small, because thapsigargin had little effect on the $[Ca^{2+}]_c$ rhythm. On the other hand, 5 μM ryanodine had a biphasic effect on Ca^{2+} mobilization, with an immediate increase and successive decrease in $[Ca^{2+}]_c$. Ryanodine facilitates Ca^{2+} release from ryanodine-sensitive internal Ca^{2+} stores at low concentrations (10–100 nM) and inhibits its Ca^{2+} release at high concentrations (1–100 μM) (Sabbadin et al., 1992; Hatem et al., 1995). The biphasic effect of ryanodine observed in the present study, therefore, may be due to the gradual diffusion of ryanodine to SCN neurons plated on the collagen gel sheet. The involvement of ryanodine-sensitive Ca^{2+} stores in the circadian $[Ca^{2+}]_c$ rhythms was further confirmed by an inhibitor for ryanodine-sensitive Ca^{2+} stores, 8-Br-cADPR (Walseth and Lee, 1993; Reyes-Harde et al., 1999). Ryanodine-receptor-mediated Ca^{2+} mobilization depends on $[Ca^{2+}]_c$ and thus can contribute to signal amplification (i.e., Ca^{2+}-induced Ca^{2+} release). Therefore, the initial Ca^{2+} signals producing the circadian variations in the Ca^{2+} release from internal stores remain to be identified. Type-2 ryanodine receptors are expressed in the SCN, and a circadian rhythm has been demonstrated in the B_{max} for ryanodine binding, but not IP_3 binding (Diaz-Munoz et al., 1999). Peak ryanodine binding occurs early in the subjective daytime (CT 1–4). Thus, the activity and/or expression of the ryanodine receptor itself may be one mechanism underlying the circadian $[Ca^{2+}]_c$ rhythm.

The Action Potential Firing Rhythms Have Little Effect on the $[Ca^{2+}]_c$ Rhythms

The majority of SCN neurons exhibited a circadian oscillation in $[Ca^{2+}]_c$ that was advanced from or out-of-phase with the MUA rhythm. To analyze the involvement of synaptic interactions in these $[Ca^{2+}]_c$ rhythms and the contribution of Ca^{2+} influx through the voltage-sensitive Ca^{2+} channels to the generation of circadian $[Ca^{2+}]_c$ rhythms, we examined the effects of TTX and nimodipine. TTX did not inhibit the $[Ca^{2+}]_c$ rhythms, including anti-phase $[Ca^{2+}]_c$ rhythms observed in a few SCN neurons (Figure 3D). These results demonstrate that the observed circadian $[Ca^{2+}]_c$ rhythms are not dependent on synaptic interactions but are cell autonomous. Nimodipine and TTX strongly suppressed the MUA rhythm, consistent with observations in rat SCN neurons (Pennartz et al., 2002). Neither nimodipine nor TTX, however, had significant effects on the circadian $[Ca^{2+}]_c$ rhythms. Although nimodipine is a selective L-type Ca^{2+} channel blocker and the L-type Ca^{2+} channel is not the sole voltage-sensitive Ca^{2+} channel expressed in SCN neurons, the results suggest that voltage-dependent Ca^{2+} influx through the plasma membrane is not a major determinant of $[Ca^{2+}]_c$ rhythms.

The presence of circadian variation in $[Ca^{2+}]_c$ is consistent with what Colwell (2000) observed in acute SCN slices using fura-2AM. A lack of effect of TTX and nimodipine on $[Ca^{2+}]_c$, however, is clearly different from what Colwell (2000) reported. The fura-2AM experiments distinguish neither neurons and glial cells nor rhythmic and nonrhythmic neurons, and all $[Ca^{2+}]_c$ values were averaged across different slices. This averaging of different cells will increase the variability of the $[Ca^{2+}]_c$ measurements and may cause the above discrepancy. Also, this explains why we did not observe a circadian $[Ca^{2+}]_c$ rhythm in the acute SCN slices in our previous study using fura-2AM (Ikeda, et al., 2003). To address technical limitations of fura-2AM experiments, the present study used a fluorescent protein Ca^{2+} indicator, cameleon,

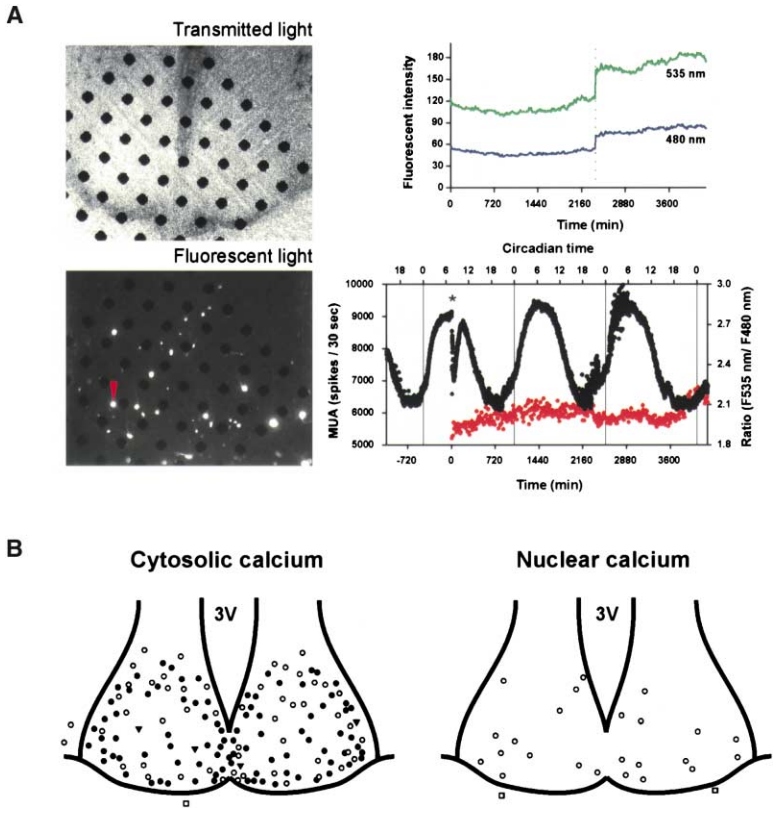

Figure 5. Long-Term Nuclear Ca^{2+} Imaging on the Multiple Electrode Array

(A) The SCN slice was transfected with a nucleus-targeted cameleon cDNA and cultured on a MEAD. Images (left) of a living SCN slice cultured on a MEAD with transmitted light (top) and fluorescent light (bottom). An example time course of nucleus-targeted cameleon fluorescence was plotted on the right. Details are as in Figure 2B. There was no circadian rhythm in the nuclear Ca^{2+} concentration (red), while there was circadian MUA rhythm (black).

(B) Approximate location of neurons in which the long-term Ca^{2+} dynamics were analyzed using either untargeted cameleon (left) or nucleus-targeted cameleon (right). All SCN slices demonstrated circadian MUA rhythms. Open circles, neurons exhibiting no circadian Ca^{2+} rhythm; open squares, glial cells exhibiting no circadian Ca^{2+} rhythm; closed circles, neurons exhibiting circadian Ca^{2+} rhythms; closed triangles, neurons exhibiting antiphase circadian Ca^{2+} rhythms. Two neurons located outside of the SCN had no circadian rhythms in $[Ca^{2+}]_c$.

and clearly demonstrated the presence of a circadian $[Ca^{2+}]_c$ rhythm in SCN neurons that is not dependent on the action potential firing rhythms.

Circadian $[Ca^{2+}]_c$ Rhythms Could Indirectly Modulate Action Potential Firing Rhythms

The $[Ca^{2+}]_c$ near the plasma membrane may modulate action potential firing rapidly and directly through Ca^{2+}-activated K^+ channels in SCN neurons (Walsh et al., 1995). Two observations, however, suggest that the observed circadian $[Ca^{2+}]_c$ rhythm is not directly driving the MUA rhythms: (1) the $[Ca^{2+}]_c$ rhythm peaks preceded the MUA rhythm peaks by 4.4 $\pm$ 0.2 hr on average, and (2) inhibitors of ryanodine-sensitive Ca^{2+} stores only produced a partial reduction in the MUA rhythm. Thus, it is likely that there are multiple intermediate steps coupling the Ca^{2+} and MUA rhythm or they are independently driven. Possible intermediates include the Ca^{2+}-sensitive enzymes, such as the Ca^{2+}/calmodulin-dependent protein kinases (CaMK), that may be rhythmically activated by the $[Ca^{2+}]_c$ rhythm. These enzymes then could phosphorylate voltage-gated ion channels including L-type Ca^{2+} channels and modulate action potential firing frequencies in SCN neurons (Jiang et al., 1997; Pennartz et al., 2002).

NMDA-induced Ca^{2+} influx together with ryanodine-receptor mediated amplification of Ca^{2+} signals are thought to be a trigger for circadian phase delays at the second messenger level (Ding et al., 1994, 1998). Rapid gene transcription of *mPer1* and *mPer2* following the CaMK-dependent phosphorylation of the cAMP response element binding protein (CREB) is the proposed downstream signaling pathway for the NMDA-induced phase shifts (Ginty et al., 1993; Ding et al., 1997; von Gall et al., 1998; Yokota et al., 2001). The circadian $[Ca^{2+}]_c$ rhythm observed in the present study precedes the reported peak of *mPer1* and *mPer2* transcription rhythms by several hours (Albrecht et al., 1997; Shigeyoshi et al., 1997; Jin et al., 1999). Thus, this raises the possibility that circadian release of Ca^{2+} from ryanodine-sensitive stores may interact with the proposed CREB-mediated regulation of clock gene transcription and modulate the MUA rhythms.

Differential Regulation of Cytosolic and Nuclear Ca^{2+} Concentration in SCN Neurons

Most of the Ca^{2+}-dependent intracellular signaling processes are regulated in the cytosol, but one of the CaMK subtypes, CaMK IV, is localized in the neuronal nucleus and plays a critical role in CREB phophorylation (Bito et al., 1996; Deisseroth et al., 1996). The CaMK IV immunoreactivity has been shown in the SCN (Nakamura et al., 1995). Together with the present results showing the NMDA-induced nuclear Ca^{2+} mobilization (Figure 4), it is reasonable to consider that the nuclear Ca^{2+} response in SCN neurons might be important for circadian regulation.

We have shown that orphanin-FQ receptors activate K^+ channels, reduce the baseline $[Ca^{2+}]_c$, inhibit the NMDA-induced Ca^{2+} influx in SCN neurons, and inhibit light-induced behavioral phase shifts (Allen et al., 1999). The present study further demonstrated that orphanin-FQ reduced the baseline and NMDA-induced changes in $[Ca^{2+}]_c$, having little effect on nuclear Ca^{2+} concentra-

tion. These results demonstrate that Ca^{2+} concentrations in the nucleus and cytosol of SCN neurons differ in their response to receptor activation, and the source of the increase in nuclear Ca^{2+} concentration is not simple diffusion from the cytosol. The observation that there were no significant effects of orphanin-FQ on the NMDA-induced nuclear Ca^{2+} response may be due to the fact that in the present experiments NMDA receptors were pharmacologically stimulated (100 μM NMDA with a reduced extracellular Mg^{2+} concentration), which may have activated Ca^{2+}-induced Ca^{2+} release to maximal levels. Under physiological conditions, Ca^{2+} permeability through NMDA receptors (Pennartz et al., 2001; Ikeda et al., 2003), linking voltage-dependent Ca^{2+} channels, or ryanodine receptor-mediated Ca^{2+}-induced Ca^{2+} release together with regulation of membrane excitability by other neurotransmitter receptors may synergistically determine the magnitude of the nuclear Ca^{2+} response.

The baseline nuclear Ca^{2+} concentration was lower than baseline $[Ca^{2+}]_c$ and did not exhibit circadian oscillations. The compartmentalization of cytosolic and nuclear Ca^{2+} has been described in several cell types. For example, nuclear Ca^{2+} concentration estimated using fura-2 is twice $[Ca^{2+}]_c$ in smooth muscle cells (Williams et al., 1985). Also, using nucleus-targeted and untargeted aequorin, Badminton et al. (1995) demonstrated a smaller Ca^{2+} response in the nucleus than that in the cytosol of COS7 cells, suggesting nuclear Ca^{2+} barriers. In contrast, Brini et al. (1993, 1994) used aequorin and demonstrated almost identical Ca^{2+} concentration in the cytosol and nucleus of HeLa cells. Therefore, Ca^{2+} gradients between the nucleus and cytosol may depend on the types of cell and stimulants used in the experiments. Interestingly, Wood et al. (2001) used aequorin expressed in tobacco seedlings and reported circadian rhythms in $[Ca^{2+}]_c$, but not in nuclear Ca^{2+} concentration. Although Ca^{2+} homeostasis and its regulation in plant cells are different from those in mammalian cells, a stable nuclear Ca^{2+} concentration across circadian cycles may be common for a wide variety of cells.

The present results also demonstrated the presence of calbindin and calretinin in SCN slice cultures of mice. Both of these Ca^{2+} binding proteins have high affinity for Ca^{2+} (K_d = 300 nM for calbindin and 250 nM for calretinin; Cheung et al., 1993) close to the range of $[Ca^{2+}]_c$ estimated in the present study. The molecular size of these Ca^{2+} binding proteins is small enough to distribute in the nucleus as well as in the cytosol. Therefore, these Ca^{2+} binding proteins may buffer both cytosolic and nuclear Ca^{2+}. In the hamster SCN, calbindin expression is limited to a subpopulation of SCN neurons, which is hypothesized to have a critical role in the generation of behaviors regulated by circadian rhythms (LeSauter and Silver, 1999). The high-capacity Ca^{2+}-buffering system in SCN neurons may prevent undesirable phase shifts via general levels of neuronal excitation and contribute to the stabilization of circadian oscillations.

Possible Role of $[Ca^{2+}]_c$ Rhythms as an Output Signal for the Circadian Clock

The mammalian circadian clock system consists of three conceptual components, (1) the core oscillator composed of gene transcription feedback loops, (2) input (i.e., resetting) pathways conveying environmental time cues to the oscillator, and (3) output pathways by which the oscillator drives action potential firing rhythms, rhythmic transmitter release, and ultimately circadian oscillations of diverse physiological activity and behaviors. Involvement of L-type Ca^{2+} channels (Pennartz et al., 2002) and ryanodine receptor-mediated Ca^{2+} release from internal stores (the present results) in action potential firings demonstrate cytosolic Ca^{2+} as an important intracellular messenger for output pathways via neuronal circuits (Aston-Jones et al., 2001). Transplantation of isolated SCN grafts can entrain circadian behavior in SCN-lesioned hosts, and thus, diffusible factors released from SCN neurons may be sufficient output signals (Silver et al., 1996). In general, neurotransmitter release is highly dependent on $[Ca^{2+}]_c$, and thus, circadian rhythmicity observed in $[Ca^{2+}]_c$ may also be an important intracellular step in the humoral output pathway from SCN neurons.

Experimental Procedures

SCN Slice Culture

Slice cultures were prepared from the SCN of 3-day-old mice (C57BL/6). Coronal hypothalamic slices containing the SCN were cut using a vibrating-blade microtome in artificial cerebrospinal fluid (ACSF) containing 138.6 mM NaCl, 3.35 mM KCl, 21 mM $NaHCO_3$, 0.6 mM NaH_2PO_4, 9.9 mM d-glucose, 0.5 mM $CaCl_2$, and 3 mM $MgCl_2$, that was filtered through a 0.22 μm membrane filter and bubbled with 95% O_2 and 5% CO_2. Three or four sequential slices (350 μM) were cut from the rostral to the caudal brain starting at the rostral end of the anterior commissure. These slices were trimmed to an approximately 4 × 4 mm square containing the ventral end of the hypothalamus centered on the third ventricle. The slices were placed in a 0.40 μm filter cup (Millicell-CM, Millipore, Bedford, MA). All these procedures were completed within 15 min at 4°C under sterile conditions. The filters were placed in a standard 6-well plate and cultured with 1 ml of medium consisting of 50% Eagle's basal medium, 25% Earle's balanced salt solution, and 25% heat-inactivated horse serum supplemented with 5 mg/ml glucose and 1:100 Glutamax (GIBCO BRL). The cultures were maintained in a CO_2 incubator at 35.5°C ± 0.5°C and 5% CO_2. The medium was changed every 3–4 days. The slice containing the rostrocaudal center of the SCN was used for further experiments. The Institutional Animal Care and Use Committee approved all procedures involving animals.

Construction and Transfection of the Cameleon Expression Vectors

Nucleus-targeted and untargeted yellow cameleon 2.1 expression vectors (Miyawaki et al., 1997, 1999) were used with the following modifications. The cameleon used (YC2.1) was constructed with cyan-shifted and yellow-shifted green fluorescent proteins linked to opposite ends of the Ca^{2+} binding region of calmodulin, yielding a significant decrease in sensitivity to pH (Miyawaki et al., 1999). A HindIII-EcoRI fragment containing the cDNA encoding cameleon was isolated and subcloned into HindIII- and EcoRI-digested pBluescriptII (Stratagene, La Jolla, CA). For neuron-specific expression, the 5′-flanking sequence (2.7 kb) with exon 1 and intron 1 of rat neuron-specific enolase genomic DNA and SV40 polyadenylation signals from pRc/RSV (Invitrogen, Carlsbad, CA) were ligated into the HindIII and EcoRI site of pBluescriptII containing the cameleon gene. Gold particles (0.6 μm, 5 mg) were coated with cameleon expression vector (20 μg) according to the manufacturer's instructions and blasted into 7- to 9-day-old cultures with helium pressure (195 psi) using the Helios Gene Gun system (BioRad Laboratories, Hercules, CA). Expression of cameleon protein in SCN neurons was estimated by the increasing fluorescence intensity in individual neurons that became maximal 3–5 days after transfection. Although the level of cameleon fluorescence was stable for up to 1 month, all Ca^{2+} imaging experiments were performed within 15 days of transfection.

Immunohistochemistry

To characterize the cultured slices, single-step triple immunofluorescent staining was performed using antibodies against GAD65, calbindin D28k, and calretinin. The slice culture was fixed with 4% paraformaldehyde in phosphate-buffered saline (PBS) at pH 7.4 for 20 min and removed from the membrane filter. The samples were rinsed three times with PBS and incubated in 10% donkey serum (Jackson ImmunoResearch Laboratories, West Grove, PA) in 0.5% Triton-X (Sigma) PBS for 2 hr at room temperature to block nonspecific antibody binding. Samples were then incubated overnight at 4°C with 1:200 mouse anti-GAD65, 1:1000 rabbit anti-calbindin, and 1:1000 goat anti-calretinin antibodies (Chemicon International Inc., Temecula, CA) dissolved in 5% donkey serum and 0.5% Triton-X PBS. Following three 20 min rinses of the tissue with PBS, the samples were incubated with secondary antibodies (1:200 Cy3-conjugated donkey anti-rabbit IgG, 1:200 FITC-conjugated donkey anti-goat IgG, and 1:200 AMCA-conjugated donkey anti-mouse IgG; Jackson) overnight at 4°C. Following four 20 min rinses, the samples were mounted on microscope slides. The validity of the triple staining method was confirmed by consecutively staining for calbindin, calretinin, and GAD65. No cross-reactivity of the primary and secondary antibodies was observed at the above concentrations. Other cultures were stained with antibodies against MAP2 and GFAP using a two-step staining method as follows. The fixed slices were rinsed and incubated with 1:200 mouse anti-MAP2 antibody (Sigma) dissolved in 5% donkey serum and 0.5% Triton-X PBS overnight at 4°C. Following three 20 min rinses of the antibody solution with PBS, the sample was incubated with AMCA-conjugated donkey anti-mouse IgG (1:200) overnight at 4°C. Following three 20 min rinses with PBS, the sample was incubated with 1:200 Cy3-conjugated mouse anti-GFAP (Sigma). Following four 20 min rinses with PBS, the slice was embedded in 3% low-temperature-melting agar, transected using a vibrating-blade microtome into 150 μm thick slices, and mounted on microscope slides.

The fluorescent images were viewed and processed using an inverted microscope (DM IRBE2, Leica, Deerfield, IL) with an objective lens (Plan Achromat ×10/0.25 or PLFLUOTAR ×20/0.5), a Micromax camera (Princeton Instruments, Monmouth Junction, NJ), and MetaMorph ver. 4.1 software (Universal Imaging, West Chester, PA).

Replating SCN Slices on the MEAD

Microelectrode arrays containing 64 electrodes, each 50 × 50 μm, arranged in an 8 × 8 pattern with 150 μm gaps (MED-P5151, Panasonic, Osaka, Japan) or 20 × 20 μm with 100 μm gaps (MED-P210A, Panasonic), were used. The electrical characteristics of the MEAD and its applicability in recording from SCN neurons have been previously described (Honma et al., 1998; Oka et al., 1999). The MEAD was sterilized with 70% ethanol and 15 min exposure to UV light and was coated with pig collagen (Cellmatrix type 1-c, Nitta Gelatin, Osaka, Japan). The collagen-coated MEAD was filled with 2 ml of culture medium and placed in a 100 mm petri dish containing 6 ml sterile water to humidify the atmosphere.

Hypothalamic slice cultures containing the center of the SCN and with successful cameleon expression were placed onto the MEADs. The membrane filter beneath the SCN slice was carefully cut to the size of the tissue, and the upper surface of the slice was placed down on the MEAD. The slice position was adjusted to ensure that the SCN was over the electrode array during a gradual reduction of the culture medium volume to approximately 150 μl. The culture was maintained in a CO_2 incubator, and 130 μl medium was exchanged every 18–36 hr. The shape of cameleon-expressing neurons did not change during or after this replating procedure. A stable SCN structure on the MEAD was also confirmed with immunostaining with a GAD65 antibody after 2 weeks culture on the MEAD.

Recording of MUA Rhythms

MUA was recorded from SCN slice cultures plated on the MEAD. The MEAD was connected to an input amplifier (SH-MED8, Panasonic) through a MEAD connector (SACC-1, Panasonic) located on a custom-built microscope stage CO_2 incubator. The incubator consisted of a 20 × 30 cm iron base and an aluminum block through which the temperature was controlled using a bath-temperature controller (DTC-200T, DIA MEDICAL SYSTEM, Tokyo, Japan). A water bath on the iron base provided high humidity, and gentle CO_2 bubbling through the water bath adjusted the CO_2 concentration to approximately 5%. The electronic signals from the input amplifier were further amplified by an eight-channel amplifier (MEG6180, Nihon Kohden, Tokyo, Japan), and the outputs fed to a digital storage oscilloscope (VC-6523, Hitachi, Tokyo, Japan) and an eight-channel digitizer (EN-601J, Nihon Kohden, Tokyo, Japan). The analog spikes were converted to digital (+5V) pulses, and the output signal fed into a laptop computer through a 24 point TTL input card (PIO-24W PM, Contec, Tokyo, Japan). The MUA frequencies were calculated at 30 s intervals and displayed on the computer screen using software written by M.I.

Ca^{2+} Imaging

During the recording of MUA from the SCN, cameleon fluorescence from SCN neurons was observed using an inverted microscope (IMT-2, Olympus), a mercury short arc lamp, an excitation filter (435.8 nm DF10, Omega Optical, Brattleboro, VT), an excitation neutral density filter (ND.5, Omega Optical), a dichroic mirror (455DRLP, Omega Optical), and a 20× objective lens (LWD CDPlan 20PL, NA0.4, Olympus). The two emission bandpass filters (480DF30 and 535DF25, Omega Optical) were switched with a filter changer wheel (C4312, Hamamatsu Photonics, Hamamatsu, Japan), and the image pairs, each accumulated for eight video frames, were exposed to a charge-coupled-device (CCD) camera (C2400, Hamamatsu) through an image intensifier (M4314, Hamamatsu) at 10 min intervals. An electromagnetic shutter (Copal, Tokyo, Japan) was set in front of the lamp house to reduce bleaching of cameleon fluorescence during sampling intervals. The shutter, filter changer wheel, and image acquisition were regulated using Argus50CA imaging software (Hamamatsu) installed on a microcomputer.

The NMDA-induced Ca^{2+} increase in single SCN neurons was observed using an upright microscope (Axioskop FS, Carl Zeiss) with a water immersion objective (Achroplan 63× NA0.95, Carl Zeiss). A SCN slice was cut from a filter cup and transferred into the microscope chamber. The slice was perfused with ACSF containing 1 μM TTX, 2.5 mM $CaCl_2$, and 0.5 mM $MgCl_2$ that was bubbled with 95% O_2 and 5% CO_2 for at least 30 min prior to the experiments. The SCN neurons were exposed to 440 ± 5 nm light using a monochromator (Polychrome 2; Till Photonics, Martinsried, Germany) with a bandpass filter (440NBD10, Omega Optical). The resultant fluorescence image was separated using a dichroic mirror (455DRLP; Omega Optical) and fed into double-view optics (A4313, Hamamatsu), in which one image was split into bilateral images via internal reflection mirrors and processed using two dichroic mirrors (515 DRLPXR; Omega Optical) and bandpass filters (480DF30 and 535DF25 filters). The monochromator and the CCD camera were controlled using digital imaging software (ARGUS HiSCA; Hamamatsu). NMDA (Sigma) and orphanin-FQ (a gift from Dr. D.K. Grandy, Oregon Health & Science University) were applied via the perfusate.

Statistical Analyses

The circadian amplitude and period of the MUA and $[Ca^{2+}]_c$ rhythms were calculated using a four-parameter sine curve fitting using Sigma Plot ver.4.01 software (SPSS Inc., Chicago, IL). The calculated amplitude and period before drug applications were regarded as control values. Amplitudes less than three standard deviations above the baseline noise (fluctuations of ten data points) were regarded as no circadian rhythm. The CT was calculated from the control MUA rhythms, although no significant phase shifts were produced in these rhythms by the drug treatments. The peak MUA was defined as CT 6, and the trough was defined as CT 18. Amplitudes were compared using the two-tailed, paired t test. The mean cytosolic and nuclear Ca^{2+} concentrations were compared using the two-tailed, unpaired t test.

Acknowledgments

We thank Drs. Gary Banker (Oregon Health & Science University) and Sato Honma (Hokkaido University) for their advice on neuronal cell cultures and MEAD recordings. The neuron-specific enolase promoter was a gift from Dr. Kenji Sakimura (Nigata University). This work is supported in part by a grant from the NIH (NS036607) to

C.N.A., a grant for Research for the Future Program (96L00310) from Japan Society for the Promotion of Science to T.Y., a grant-in-aid for scientific research (B14380372) from the Ministry of Education, Culture, Sports, Science and Technology Japan to M.I., and a grant from Ono Pharmaceutical Company to C.N.A, M.I., and T.Y.

Received: July 26, 2002
Revised: February 21, 2003
Accepted: March 19, 2003
Published: April 23, 2003

References

Albrecht, U., Sun, Z.S., Eichele, G., and Lee, C.C. (1997). A differential response of two putative mammalian circadian regulators, *mper1* and *mper2*, to light. Cell *91*, 1055–1064.

Allen, C.N., Jiang, Z.G., Teshima, K., Darland, T., Ikeda, M., Nelson, C.S., Quigley, D.I., Yoshioka, T., Allen, R.G., Rea, M.A., and Grandy, D.K. (1999). Orphanin-FQ/nociceptin (OFQ/N) modulates the activity of suprachiasmatic nucleus neurons. J. Neurosci. *19*, 2152–2160.

Aston-Jones, G., Chen, S., Zhu, Y., and Oshinsky, M.L. (2001). A neural circuit for circadian regulation of arousal. Nat. Neurosci. *4*, 732–738.

Badminton, M.N., Kendall, J.M., Sala-Newby, G., and Campbell, A.K. (1995). Nucleoplasmin-targeted aequorin provides evidence for nucleus calcium barrier. Exp. Cell Res. *216*, 236–243.

Belenky, M., Wagner, S., Yarom, Y., Matzner, H., Cohen, S., and Castel, M. (1996). The suprachiasmatic nucleus in stationary organotypic culture. Neuroscience *70*, 127–143.

Bito, H., Deisseroth, K., and Tsein, R.W. (1996). CREB phosphorylation and dephosphorylation: a Ca^{2+}- and stimulus duration-dependent switch for hippocampal gene expression. Cell *87*, 1203–1214.

Brini, M., Murgia, M., Pasti, L., Picard, D., Pozzan, T., and Rizzuto, R. (1993). Nuclear Ca^{2+} concentration measured with specifically targeted recombinant aequorin. EMBO J. *12*, 4813–4819.

Brini, M., Marsault, R., Bastianutto, C., Pozzan, T., and Rizzuto, R. (1994). Nuclear targeting of aequorin. A new approach for measuring nuclear Ca^{2+} concentration in intact cells. Cell Calcium *16*, 259–268.

Cheung, W.T., Richards, D.E., and Rogers, J.H. (1993). Calcium binding by chick calretinin and rat calbindin D28k synthesised in bacteria. Eur. J. Biochem. *215*, 401–410.

Colwell, S. (2000). Circadian modulation of calcium levels in cells in the suprachiasmatic nucleus. Eur. J. Neurosci. *12*, 571–576.

de la Mora, M.P., Possani, L.D., Tapia, R., Terán, L., Palacios, R., Fuxe, K., Hókfelt, T., and Ljungdhal, Å. (1981). Demonstration of gamma-aminobutyrate-containing nerve terminals by means of antibodies against glutamate decarboxylase. Neuroscience *6*, 875–895.

Deisseroth, K., Bito, H., and Tsien, R.W. (1996). Signaling from synapse to nucleus: postsynaptic CREB phosphorylation during multiple forms of hippocampal synaptic plasticity. Neuron *16*, 89–101.

Diaz-Munoz, M., Dent, M.A., Granados-Fuentes, D., Hall, A.C., Hernandez-Cruz, A., Harrington, M.E., and Aguilar-Roblero, R. (1999). Circadian modulation of the ryanodine receptor type 2 in the SCN of rodents. Neuroreport *10*, 481–486.

Ding, J.M., Chen, D., Iber, E.T., Faiman, L.E., Rea, M.A., and Gillette, M.A. (1994). Resetting the biological clock: mediation of nocturnal circadian shifts by glutamate and NO. Science *266*, 1713–1717.

Ding, J.M., Faiman, L.E., Hurst, W.J., Kuriashkina, L.R., and Gillette, M.A. (1997). Resetting the biological clock: mediation of nocturnal CREB phosphorylation via light, glutamate, and nitric oxide. J. Neurosci. *17*, 667–675.

Ding, J.M., Buchanan, G.F., Tischkau, S.A., Chen, D., Kuriashkina, L., Faiman, L.E., Alster, J.M., McPherson, P.S., Campbell, K.P., and Gillette, M.U. (1998). A neuronal ryanodine receptor mediates light-induced phase delays of the circadian clock. Nature *394*, 381–384.

Earnest, D.J., and Sladek, C.D. (1986). Circadian rhythms of vasopressin release from individual rat suprachiasmatic explants in vitro. Brain Res. *382*, 129–133.

Ginty, D.D., Kornhauser, J.M., Thompson, M.A., Banding, H., Mayo, K.E., Takahashi, J.S., and Greenberg, M.E. (1993). Regulation of CREB phosphorylation in the suprachiasmatic nucleus by light and a circadian clock. Science *260*, 238–241.

Green, D.J., and Gillette, R. (1982). Circadian rhythm of firing rate recorded from single cells in the rat suprachiasmatic brain slice. Brain Res. *245*, 198–200.

Hatem, S.N., Sweeten, T., Vetter, V., and Morad, M. (1995). Evidence for presence of Ca^{2+} channel-gated Ca^{2+} stores in neonatal human arterial myocytes. Am. J. Physiol. *268*, H1195–H1201.

Herzog, E.D., Geusz, M.E., Khalsa, S.B.S., Straume, M., and Block, G.D. (1997). Circadian rhythms in mouse suprachiasmatic nucleus explants on multimicroelectrode plates. Brain Res. *757*, 285–290.

Honma, S., Shirakawa, T., Katsuno, Y., Namihira, M., and Honma, K. (1998). Circadian periods of single suprachiasmatic neurons in rats. Neurosci. Lett. *250*, 157–160.

Ikeda, M., Sugiyama, T., Suzuki, K., Moriya, T., Shibata, S., Katsuki, M., Allen, C.N., and Yoshioka, T. (2000). PLC-β4-independent Ca^{2+} rise via muscarinic receptors in the mouse suprachiasmatic nucleus. Neuroreport *11*, 907–912.

Ikeda, M., Yoshioka, T., and Allen, C.N. (2003). Developmental and circadian changes in Ca^{2+} mobilization mediated by $GABA_A$ and NMDA receptors in the suprachiasmatic nucleus. Eur. J. Neurosci. *17*, 57–70.

Inouye, S.T., and Kawamura, H. (1979). Persistence of circadian rhythmicity in a mammalian hypothalamic 'island' containing the suprachiasmatic nucleus. Proc. Natl. Acad. Sci. USA *76*, 5962–5966.

Jiang, Z.G., Yang, Y.Q., Liu, Z.P., and Allen, C.N. (1997). Membrane properties and synaptic inputs of the suprachiasmatic nucleus neurons in rat brain slices. J. Physiol. *499*, 141–159.

Jin, X., Shearman, L.P., Weaver, D.R., Zylka, M.J., de Vries, G.J., and Reppert, S.M. (1999). A molecular mechanism regulating rhythmic output from the suprachiasmatic circadian clock. Cell *96*, 57–68.

Johnson, C.H., Knight, M.R., Kondo, T., Masson, P., Sedbrook, J., Haley, A., and Trewavas, A. (1995). Circadian oscillation of cytosolic and chloroplastic free calcium in plants. Science *269*, 1863–1865.

Kerr, R., Lev-Ram, V., Baird, G., Vincent, P., Tsien, R.Y., and Schafer, W.R. (2000). Optical imaging of calcium transients in neurons and pharyngeal muscle of *C. elegans*. Neuron *26*, 583–594.

Kopp, M.D., Schomerus, C., Dehghani, F., Korf, H.W., and Meissl, H. (1999). Pituitary adenylate cyclase-activating polypeptide and melatonin in the suprachiasmatic nucleus: effects on the calcium signal transduction cascade. J. Neurosci. *19*, 206–219.

LeSauter, J., and Silver, R. (1999). Localization of a suprachiasmatic nucleus subregion regulating locomotor rhythmicity. J. Neurosci. *19*, 5574–5585.

Miyawaki, A., Llopis, J., Heim, R., McCaffery, J.M., Adams, J.A., Ikura, M., and Tsien, R.Y. (1997). Fluorescent indicators for Ca^{2+} based on green fluorescent proteins and calmodulin. Nature *388,* 882–887.

Miyawaki, A., Griesbeck, O., Heim, R., and Tsien, R.Y. (1999). Dynamic and quantitative Ca^{2+} measurements using improved cameleons. Proc. Natl. Acad. Sci. USA *96*, 2135–2140.

Moore, R.Y., and Eichler, V.B. (1972). Loss of a circadian adrenal corticosterone rhythm following suprachiasmatic lesions in the rat. Brain Res. *42*, 201–206.

Moore, R.Y., and Speh, J.C. (1993). GABA is the principal neurotransmitter of the circadian system. Neurosci. Lett. *150*, 112–116.

Nakamura, Y., Okuno, S., Sato, F., and Fujisawa, H. (1995). An immunohistochemical study of Ca^{2+}/calmodulin-dependent kinase IV in the rat central nervous system: light and electron microscopic observations. Neuroscience *68*, 181–194.

Oka, H., Shimono, K., Ogawa, R., Sugihara, H., and Taketani, M. (1999). A new planar multielectrode array for extracellular recording: application to hippocampal acute slice. J. Neurosci. Methods *93*, 61–67.

Pennartz, C.M., Hamstra, R., and Geurtsen, A.M. (2001). Enhanced NMDA receptor activity in retinal inputs to the rat suprachiasmatic nucleus during the subjective night. J. Physiol. *532*, 181–194.

Pennartz, C.M., de Jeu, M.T., Bos, N.P., Schaap, J., and Geurtsen,

A.M. (2002). Diurnal modulation of pacemaker potentials and calcium current in the mammalian circadian clock. Nature *416*, 286–290.

Reyes-Harde, M., Empson, R., Potter, B.V., Galione, A., and Stanton, P.K. (1999). Evidence of a role for cyclic ADP-ribose in long-term synaptic depression in hippocampus. Proc. Natl. Acad. Sci. USA *96*, 4061–4066.

Sabbadin, R.A., Betto, R., Teresi, A., Fachechi-Cassano, G., and Salviat, G. (1992). The effects of sphingosine on sarcoplasmic reticulum membrane calcium release. J. Biol. Chem. *267*, 15475–15484.

Sakimura, K., Kushiya, E., Ogura, A., Kudo, Y., Katagiri, T., and Takahashi, Y. (1995). Upstream and intron regulatory regions for expression of the rat neuron-specific enolase gene. Brain Res. Mol. Brain Res. *28*, 19–28.

Shearman, L.P., Sriam, S., Weaver, D.R., Maywood, E.S., Chaves, I., Zheng, B., Kume, K., Lee, C.C., van der Horst, G.T., Hastings, M.H., and Reppert, S.M. (2000). Interacting molecular loops in the mammalian circadian clock. Science *288*, 1013–1019.

Shigeyoshi, Y., Taguchi, K., Yamamoto, S., Takekida, S., Yan, L., Tei, H., Moriya, T., Shibata, S., Loros, J.J., Dunlap, J.C., and Okamura, H. (1997). Light-induced resetting of mammalian circadian clock is associated with rapid induction of *mPer1* transcript. Cell *91*, 1043–1053.

Shinohara, K., Honma, S., Katsuno, Y., Katsuno, Y., Abe, H., and Honma, K. (1995). Two distinct oscillators in the rat suprachiasmatic nucleus. Proc. Natl. Acad. Sci. USA *92*, 7396–7400.

Silver, R., LeSauter, J., Tresco, P.A., and Lehman, M.N. (1996). A diffusible coupling signal from the transplanted suprachiasmatic nucleus controlling circadian locomotor rhythms. Nature *382*, 810–813.

Stephan, F.K., and Zucker, I. (1972). Circadian rhythms in drinking behavior and locomotor activity of rats are eliminated by hypothalamic lesions. Proc. Natl. Acad. Sci. USA *69*, 1583–1586.

Tsuchiya, R., Yoshiki, F., Kudo, Y., and Morita, M. (2002). Cell type-selective expression of green fluorescent protein and calcium indicating protein, yellow cameleon, in rat cortical primary cultures. Brain Res. *956*, 221–229.

van den Pol, A.N. (1980). The hypothalamic suprachiasmatic nucleus of the rat: intrinsic anatomy. J. Comp. Neurol. *191*, 661–702.

von Gall, C., Duffield, G.E., Hasting, M.H., Kopp, M.D., Dehghani, F., Korf, H.W., and Stehle, J.H. (1998). CREB in the mouse SCN: a molecular interface coding the phase-adjusting stimuli light, glutamate, PACAP, and melatonin for clockwork access. J. Neurosci. *18*, 10389–10397.

Walseth, T.F., and Lee, H.C. (1993). Synthesis and characterization of antagonists of cyclic-ADP-ribose-induced Ca^{2+} release. Biochim. Biophys. Acta *1178*, 235–242.

Walsh, I.B., van den Berg, R.J., and Rietveld, W.J. (1995). Ionic currents in cultured rat suprachiasmatic neurons. Neuroscience *69*, 915–929.

Welsh, D.K., Logothetis, D.E., Meister, M., and Reppert, S.M. (1995). Individual neurons dissociated from rat suprachiasmatic nucleus express independently phased circadian firing rhythms. Neuron *14*, 697–706.

Williams, D.A., Fogarty, K.E., Tsien, R.Y., and Fredric, S.F. (1985). Calcium gradients in single smooth muscle cells revealed by the digital imaging microscope using Fura-2. Nature *318*, 558–561.

Wood, N.T., Haley, A., Viry-Moussaid, M., Johnson, C.H., van Der Luit, A.H., and Trewavas, A.J. (2001). The calcium rhythms of different cell types oscillate with different circadian phases. Plant Physiol. *125*, 787–796.

Yokota, S., Yamamoto, M., Moriya, T., Akiyama, M., Fukunaga, K., Miyamoto, E., and Shibata, S. (2001). Involvement of calcium-calmodulin protein kinase but not mitogen-activated protein kinase in light-induced phase delays and Per gene expression in the suprachiasmatic nucleus of the hamster. J. Neurochem. *77*, 618–627.